

See discussions, stats, and author profiles for this publication at: <https://www.researchgate.net/publication/268515013>

# Tunable Band Gap in Bilayer Graphene by Trimesic Acid Molecular Doping

ARTICLE *in* THE JOURNAL OF PHYSICAL CHEMISTRY C · OCTOBER 2014

Impact Factor: 4.77 · DOI: 10.1021/jp508679t

---

CITATIONS

4

READS

73

---

## 1 AUTHOR:



Farzaneh Shayeganfar  
Polytechnique Montréal

17 PUBLICATIONS 57 CITATIONS

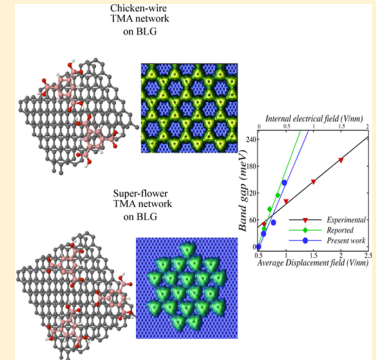
[SEE PROFILE](#)

# Tunable Band Gap in Bilayer Graphene by Trimesic Acid Molecular Doping

Farzaneh Shayeganfar\*

Engineering Physics Department and Regroupement québécois sur les matériaux de pointe (RQMP), Polytechnique Montréal, Montréal, Québec H3C 3A7, Canada

**ABSTRACT:** We are presenting the results of first-principles study of the electronic band structure properties of molecular doping of bilayer graphene with one-sided adsorption of a single and self-assembled trimesic acid (TMA) monolayer which exhibits a *p*-type dopant semiconductor. Our study demonstrates that the effect of charge transfer between the adsorbate and substrate is the origin of perturbation in inversion symmetry of bilayer graphene and a result of band gap opening. Meanwhile, doping of bilayer graphene with an organic molecule produces an internal electric (built-in) field between the bottom and top layer due to charge asymmetry. The self-assembly of trimesic acid (TMA, benzene-1,3,5-tricarboxylic acid) on bilayer graphene with the two most network arrangements improves the stability and band gap energy of the adlayer by formation of reliable hydrogen bonding. The various patterns applied to adsorption on bilayer graphene allow us to tune the induced band gap where the existence of a linear trend of energy gap with number of carriers demonstrates consistency between experimental and theoretical studies. Accordingly these data lead to further implications for nanoelectronics and nanophotonics devices.



## I. INTRODUCTION

The zero band gap makes bulk graphene unsuitable and poor for most applications. The strategy to induce and control the energy band gap in bilayer graphene is a significant development in the application of graphene in promising nanoelectronic and nanophotonic devices. Therefore, numerous research studies are considering investigation of opening a band gap in the density of states to increase applications of unique electric properties of graphene such as room temperature transistors.<sup>1–3</sup> One approach for this purpose is to impose lateral confinement of charge carriers to fabricate graphene nanostructures.<sup>4–15</sup>

The other approach is applying displacement electric fields to break the inversion symmetry in bilayer graphene, by applying an external electric field.<sup>16–20</sup> Seon-Myeong and his collaborators in their paper<sup>21</sup> explore that strain in bilayer graphene is one mechanical parameter which can produce and tune the electronic energy gap. They showed that without any external electric and gate potential the subjected layers to different strains can induce the electric fields, perpendicular to the two layers of bilayer graphene.<sup>21</sup> Hydrogenation of graphene is another strategy to tune the energy band gap opening,<sup>22</sup> while Tian and his collaborator investigated the electronic properties of adsorption of the F4-TCNQ adlayer on bilayer graphene (BLG), invoking asymmetry and an energy gap opening between two layers in BLG.<sup>23</sup>

We utilized AB-stacking of bilayer graphene for our study which has been described with a tight-binding model.<sup>24</sup> The electronic band structure of bilayer graphene is plotted in Figure 1(a), in which the pair of bands in the valence band (VB) and conduction band (CB) touch each other at the  $k$

points which is similar to the Dirac point of pristine graphene. The separation distance between two higher bands is given by  $2\gamma_1$ .<sup>24</sup> Our DFT calculations of the band structure of BLG (Figure 1a) acquire the value of  $\gamma_1$ , 0.38 eV, which is close to the reported value (0.36 eV) by Samuels and Caray in his paper.<sup>24</sup>

Previous efforts have reported the application of an external electric field to emerge asymmetry between two layers and induce band gap opening in bilayer graphene.<sup>16,25</sup> Following our previous studies on the investigation of electronic properties of adsorption of a single and self-assembled trimesic acid monolayer on graphene,<sup>26</sup> we now move to demonstrate the effect of growth of the trimesic acid layer over BLG on the electronic structure of bilayer graphene. We choose trimesic acid (TMA) which consists of three carboxylic functions (Figure 1b) where the COOH group has dual character of donor and acceptor and can form a hydrogen bond, therefore providing a perfect building block for creating stable self-assembly on graphitic surfaces.<sup>26,27</sup>

In this study, we used the *ab initio* calculation method to explore the effects of adsorption of trimesic acid (TMA) as *p*-type dopant on the top layer of BLG. We first consider and focus on the electronic properties of two adsorption sites of a single TMA molecule on bilayer graphene (Figure 1). Then we investigate the effects of a self-assembled TMA layer on bilayer graphene. We find that adsorption of trimesic acid molecules on bilayer graphene produces an internal electric field due to

Received: August 27, 2014

Revised: October 20, 2014

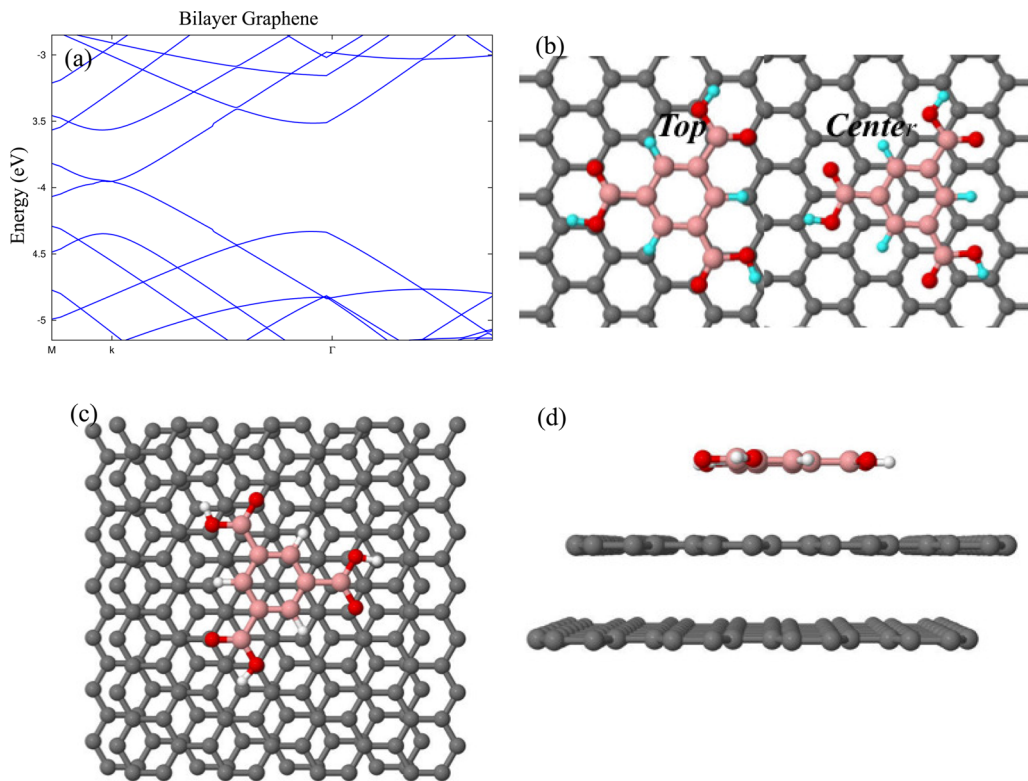


**Figure 1.** (a) Band structure of isolated bilayer graphene (BLG). (b) Two adsorption site geometries of the TMA single molecule over different arrangements of carbon atoms in top graphene layer. *Top* site represents adsorption over a hexagonal site, and *Center* is related to adsorption over a C–C bond site. Carbon atoms of the TMA molecule correspond to pink; oxygen atoms are red; and hydrogen atoms are cyan. (c) and (d) Unit cell for the adsorption of the TMA monomer on BLG.

asymmetric charge distribution between the top and bottom layers and results in band gap opening. This work elucidates the understanding of growth of ultrathin organic layers on bilayer graphene for further inspiring design of nanoelectronic devices.

## II. COMPUTATIONAL DETAILS

The structural and electronic properties have been investigated using first-principles density functional calculations by the SIESTA package.<sup>28</sup> Our first-principles calculations are based on localized basis sets (double  $\zeta$  polarized basis) with local density approximation (LDA) for exchange-correlation potential.<sup>29</sup> An appropriate Monkhorst–Pack  $k$ -point grid of  $12 \times 12 \times 1$  was used to acquire an accurate band structure and sufficient to cover the integration of the charge density. The optimization of atomic geometry and positions proceeds until the change in total energy is less than  $10^{-5}$  eV and for forces less than 0.01 eV/Å per cell.

We consider that LDA leads to a bilayer distance of 3.3 Å in good agreement with experimental observation of graphite<sup>30</sup> and can provide accurate geometry and associated electronic structure for the self-assembly of TMA as well as for its adsorption on bilayer graphene. Then, for calculating the adsorption energy of the TMA layer on bilayer graphene, we define  $E_{ad}$  via

$$E_{ad} = 1/n(E(\text{TMA}/\text{BLG}) - [E(\text{BLG}) + nE(\text{TMA})])$$

In the above,  $E(\text{TMA}/\text{BLG})$  represents the total energy for the optimized TMA layer on bilayer graphene, while  $E(\text{BLG})$  denotes the total energy for the relaxed isolated bilayer graphene.  $E(\text{TMA})$  is the total energy of an optimized isolated

(gas phase) TMA molecule, and  $n$  is the number of TMA units per cell.

All the simulated STM images were prepared with our in-house SPAGS-STM software,<sup>31</sup> and the Flex-STM module<sup>32</sup> uses a standard Hamiltonian derived from extended Hückel theory<sup>33</sup> in conjunction with the Tersoff–Hamann<sup>34</sup> level of theory to compute the tunneling current in topographic mode.

## III. RESULTS AND DISCUSSION

### III.1. TMA Single-Molecule Adsorption on Bilayer Graphene.

The optimized geometry details are listed in Table 1 with dipole moment  $p_z$ , the optimum intermolecular

**Table 1.** Electrical Dipole Moment ( $p_z$ ), Optimum Intermolecular Separation ( $d$ ), Net Charge Transfer to the TMA Molecule, and Adsorption Energy ( $E_{ad}$ ) of Two-Site Adsorption of the TMA Monomer/BLG

TMA/BLG			
$p_z$ (Debye)	$d$ (Å)	net charge ( $ e $ )	$E_{ad}$ (eV)
center	-1.19	2.83	-0.18
top	-0.93	2.92	-0.14

distance between the central TMA molecule and the top graphene in BLG, the net Mulliken charge on the adsorbate molecule, and calculated adsorption energy ( $E_{ad}$ ). In our study, we construct a different arrangement of the atoms in the adsorbate molecule over bilayer graphene: one is the *top* site (see Figure 1(b)), where TMA is commensurate with the surface, and the other is the *center* site where the TMA molecule is centered on a single atom. The trends in Table 1

represent that: (i) the *center* site is the most stable adsorption site, relevant with more favored Bernal AB stacking configuration, and (ii) the optimum intermolecular distance between hexagonal in TMA and the top graphene sheet, where  $\pi$ -electrons of carbon are concentrated, for the *top* adsorption site is placed further away with 0.10 Å relative to the *center* site. The high adsorption energies for these two adsorption sites are attributed to  $\pi-\pi$  stacking interaction.<sup>24</sup>

From the density of states (Figure 2), it can be seen that the Fermi-energy level is shifted around 0.12 eV toward the valence

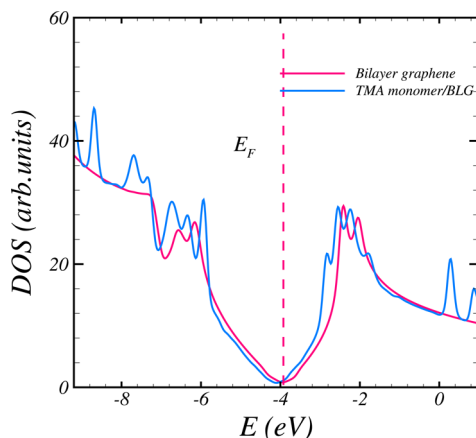


**Figure 2.** Comparison of density of states (DOS) for the TMA monolayer on BLG with isolated bilayer graphene as a reference here. There is a 0.12 eV shift for density of states of TMA/BLG below the Fermi energy of bilayer graphene.

bond (VB), and it manifests that the electrons from the VB of bilayer graphene transfer to the TMA molecule in the p-dopant adsorption process. To support our conclusion about electron withdrawal from bilayer graphene, we computed the bond length of CO for the COOH terminal upon adsorption which increases from 1.207 to 1.213 Å. The calculated Mulliken charge transfers to the TMA single-molecule adsorbate on bilayer graphene in Table 1 reveal that the TMA molecule is negatively charged as an acceptor and that the surface is donor or positively charged (p-doped).

The band structure of TMA-monomer-doped graphene (Figure 3) verifies the influence of the adlayer on the electronic band structure of bilayer graphene. The Fermi level is around 120 meV below the  $E_F$  of isolated BLG and toward the valence bond, which tells us the TMA molecular adlayer has induced p-type doping on BLG. Also at the  $k$ -point, the VB and CB

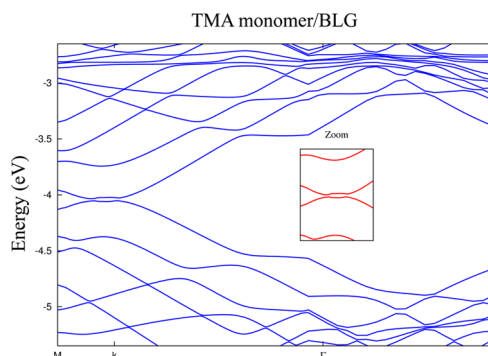


**Figure 3.** Band structure of TMA monomer/BLG.

become wider, like a “Mexican hat”,<sup>35</sup> and then the gap opening turns out to be direct band gap  $E_g$  and  $k$ -point band separation  $\Delta E_k$  as plotted in Figure 4(a).

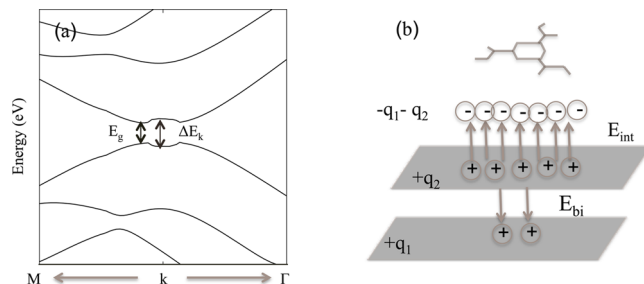


**Figure 4.** Schematic view of band gap opening principles of the TMA molecule over bilayer graphene: (a) band parameters,  $E_g$  denote the direct band gap and  $\Delta E_k$  as the band separation at the  $k$ -point and (b) interelectric ( $E_{int}$ ) and built-in electric ( $E_{bi}$ ) field in bilayer graphene with molecular doping.

Charge transfer between the TMA molecule and surface can provide crucial information on breaking of potential equivalence between the bottom- and top-layer graphene in BLG. Table 1 reports that each TMA molecule obtains near  $0.2e$  from the bilayer graphene, and it proves that the charge difference between the top and bottom layer provides a built-in electric field  $E_{bi}$  as depicted in Figure 4(b). Indeed, we figure out that the TMA adlayer attains  $q_1 + q_2$  from BLG, and hence the interelectric field  $E_{int}$  has been introduced (Figure 4(b)).

To further explore Figure 3, we calculated the direct band gap ( $E_g$ ) for monomer adsorption which is equal to 29 meV, and the  $k$ -point band separation ( $\Delta E_k$ ) is 31 meV. In view of computation of the built-in electric field,  $E_{bi}$ , the tight binding maps the relations between  $E_{bi}$ , separation distance of two BLG layers ( $d$ ), and  $k$ -point band separation as  $E_{bi} \approx (\Delta E_k/d)$ .<sup>36</sup> In our case study, by a 3.4 Å separation distance of two layers in BLG, we found the built-in electric field to be 0.09 V/nm.

**III.2. Self-Assembly of the TMA Monolayer on Bilayer Graphene.** Trimesic acid has three COOH (carboxylic) groups which are polar and both hydrogen-bonding acceptors and donors; therefore, trimesic acid offered a perfect starting point as an archetypical molecule for supramolecular self-assembly. With scanning tunneling microscopy (STM) it has been revealed that there are two network arrangements for TMA self-assembly: one is the chicken-wire net with 6-fold rings of TMA molecules and three cyclic hydrogen bonds (Figure 5(a)), and the other is a super-flower net with densely packed trimer hydrogen bonding (Figure 5(b)).<sup>27,37,38</sup> In the following section, with the main analytical tools, i.e., DFT computation, we will discuss some electronic properties such as band structure and adsorption energy for two networks of self-assembled trimesic acid structures on bilayer graphene, “chicken-wire” and “super-flower”.

**III.2.1. Adsorption of the TMA Dimer Monolayer/BLG.** To interrogate the influence of the trimesic acid layer on the electronic band structure of bilayer graphene, we construct two unit cells to model the isolated dimer and the chicken-wire network that contains 42 atoms (18C, 12H, and 12O) for the adsorbate layer, 193 carbon atoms for the substrate in the network, and 337C atoms for the isolated dimer case. To further evaluate and compare the influence of structural boundary constraints on the formation of intermolecular hydrogen bonding in self-assembled TMA, the isolated dimer

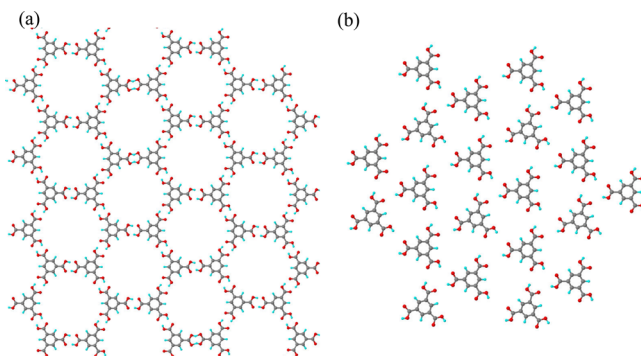


**Figure 5.** Corresponding models of (a) “chicken-wire” by three cyclic dimer hydrogen bonds and (b) “super-flower” with a trimer hydrogen bond.

adsorption on bilayer graphene is investigated (Figure 6(b)), and the unit cell is large enough to prevent the effect of neighboring cells and obtain a relevant optimized structure.

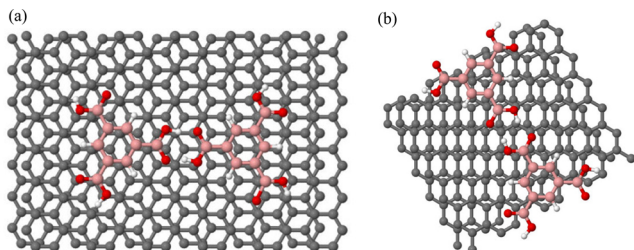


**Figure 6.** Unit cell for the adsorption of the TMA dimer monolayer on BLG, (a) in an isolated and (b) in a network TMA dimer monolayer.

To get an accurate comparison of electronic properties of the isolated dimer and 2D network (self-assembled) TMA layer on bilayer graphene, dipole moment, Mulliken charges, and adsorption energy per TMA are calculated by means of DFT computations and presented in Table 2.

**Table 2. Electrical Dipole Moment, Net Charge Transfer, and Adsorption Energy of the TMA Dimer/BLG**

	$p_z$ (Debye)	charge ( $ e $ )	$E_{ad}$ (eV)
TMA dimer(iso)/BLG	-2.23	-0.15	-3.57
TMA dimer(net)/BLG	-1.57	-0.12	-3.17

The higher stability observed for an isolated dimer compared to a single molecule can be inferred from the free COOH interaction with the surface; therefore, they can find a better optimized geometry since they have more space to move. It is worth noting that this adsorption energy is contributed from the formation of intermolecular hydrogen bonds between TMA units and stabilization energy by the surface. Compared to the network dimer adlayer (Table 2), adsorption energy for the isolated dimer is decreased from -3.57 to -3.17 eV, so correlation between dimers in the network configuration weakens the adsorption and shows minor effects of neighbors on adsorbate stability on the surface.

The band structure of the TMA dimer adsorbed on BLG (Figure 7) shows the band gap opening with an increase of TMA carrier, is enhanced, and is around 54 meV. The  $k$ -point gap is found to be 57 meV, and a built-in electric field of 0.17 V/nm is induced. The calculated band gap opening for single

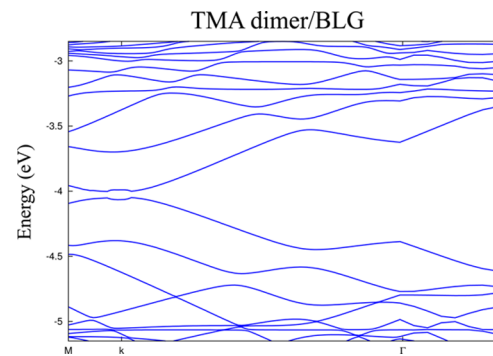


**Figure 7.** Band structure of TMA dimer/BLG in dimer network adsorption configuration.

TMA adsorption is around 29 meV, and that value increases to 54 meV for the chicken-wire network and to 78 meV for the isolated case. One plausible explanation for variation of band gap opening takes into account that the dipole moment and charge transfer between the adsorbate and surface may introduce a symmetry breaking of the  $\pi$ -states near the Fermi energy.<sup>39</sup> The value of the electric dipole in Table 2 ( $p_z$  for isolated -2.23 and for network dimer -1.57 D), from first-principle calculations, confirms that the dipole moment for various states produces a different internal electric field ( $E_{bi}$ ). The perturbation caused by this  $E_{bi}$  decreases the degeneracy degrees and forms the band gap.<sup>26</sup>

To clarify the formation of self-assembled TMA as chicken-wire-like structure on bilayer graphene, simulated topographic STM images of this structure are plotted in Figure 8, in which each ring includes three cyclic dimer hydrogen-bonding arrangements.

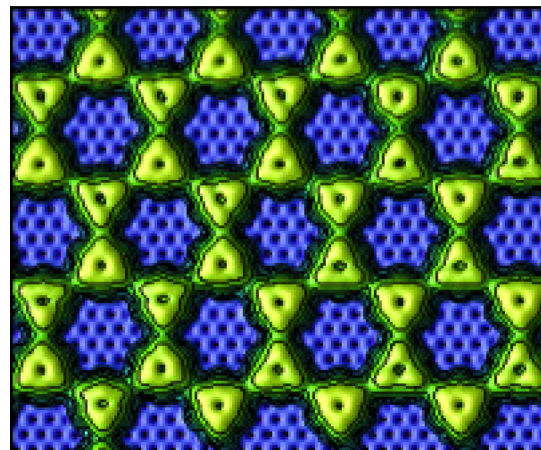


**Figure 8.** Simulated topographic STM images of chicken-wire structure are depicted and demonstrate the building blocks of cyclic dimer hydrogen-bonding networks.

**III.2.2. Adsorption of the TMA Trimer Monolayer/BLG.** As we mentioned, the TMA can create cyclic trimer hydrogen bonding as depicted in Figure 5(b). We use isolated as well as network structure (super-flower) of the TMA trimer monolayer on top of bilayer graphene to investigate some electronic properties. The molecular model of the unit cell for adsorption of the TMA monolayer on graphene is shown in Figure 9 which contains 63 atoms for the adsorbate and 256 carbon atoms for

bilayer graphene in the network and 528 C atoms for the isolated trimer case.

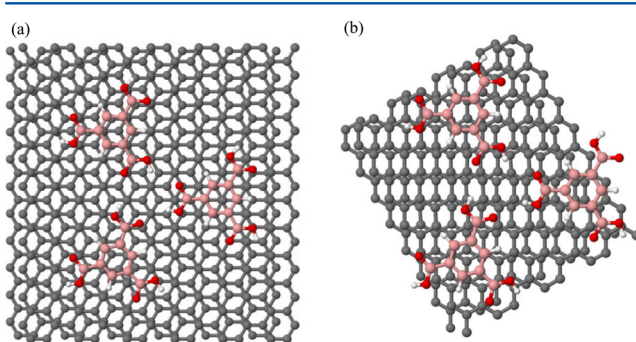


**Figure 9.** Unit cell for the adsorption of the TMA trimer monolayer on BLG, (a) in isolated and (b) in network TMA trimer adlayer.

Table 3 presents some electronic properties of the TMA trimer monolayer/BLG such as adsorption energy, the net

**Table 3. Electrical Dipole Moment, Net Charge Transfer, and Adsorption Energy of the TMA Trimer/BLG**

	$p_z$ (Debye)	net charge (lel)	$E_{ad}$ (eV)
TMA trimer(iso)/BLG	-4.61	-0.18	-3.23
TMA trimer(net)/BLG	-2.04	-0.13	-2.99

Mulliken charges acquired per TMA unit, and dipole moment. The isolated trimer adlayer adsorption energy (Table 3) is decreased from  $-3.23$  to  $-2.99$  eV compared to the network structure which is ascribed to the formation of hydrogen bonding in self-assembled TMA networks or structural boundary constraints.

The calculated band gap opening as can be seen in Figure 10 is 114 meV for the super-flower network, and the value

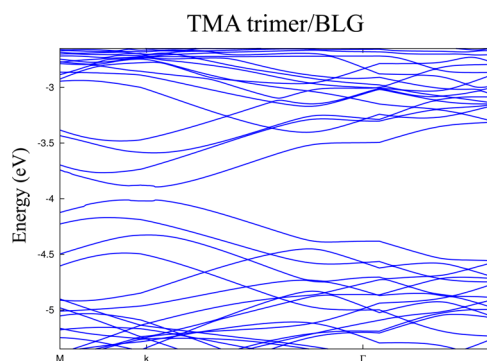


**Figure 10.** Band structure of the TMA trimer/BLG in the network adsorption configuration.

increases to 147 meV for the isolated case. The gap distance at the  $k$ -point for the network trimer is found to be 118 meV, and we find a built-in electric field of 0.35 V/nm.

The band gap opening can be attributed to perturbation of the internal electric field ( $E_{bi}$ ) which is created by molecule charge transfer between the adsorbate and substrate, and this perturbation in the system breaks the inversion symmetry of bilayer graphene.<sup>26</sup> The value of the electric dipole in Table 3 ( $p_z$  for isolated state  $-4.61$  and for network state  $-2.04$  D), from first-principle calculations, confirms that the dipole

moment for various states produces different built-in electric field and energy gap opening.<sup>26</sup> When increasing the freedom of the trimer hydrogen bonding system in an isolated arrangement, the higher stability and larger band gap as well as charge transfer originate from the increase of free interaction of COOH groups with the substrate and also reflect the propensity of forming intermolecular H-bonding in the TMA network. From these results, we conclude that by the geometry decorating of an adsorbate such as self-assembled molecules over bilayer graphene, one can tune the induced band gap in bilayer graphene. The simulated STM images of the super-flower structure on bilayer graphene, depicted in Figure 11, reveal that each carboxylic group of TMA takes part in a trimer hydrogen-bonding arrangement.

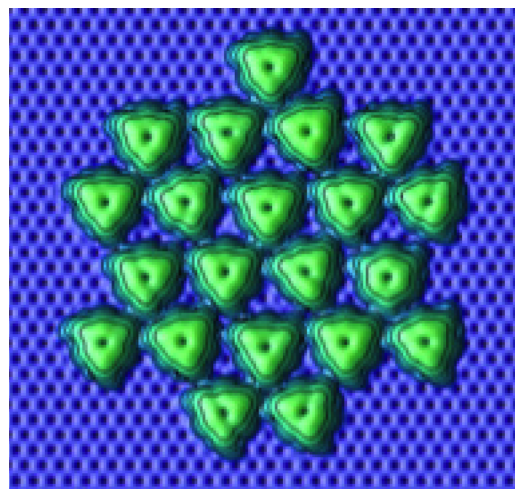


**Figure 11.** Simulated STM images of super-flower structure where each COOH terminal associates in a trimer hydrogen bonding network.

Figure 12(a) shows the evolution of the induced band gap by a number of trimesic acid units adsorbed on bilayer graphene. The figure reveals that in p-type TMA dopants studied in the present work the linear trend of directed band gap with number of TMA aggregations is in close agreement with the results of Samuels and Carey in their recent paper.<sup>24</sup> They reported that for both n-type and p-type dopants the band gap value shows ascending behavior.<sup>24</sup> It is interesting to note that we can compare the energy band gap calculated here with those reported from experimental data of dual gate devices.<sup>41</sup> By using the displacement field for the top and bottom layer in bilayer graphene, a band gap can be created and controlled, and then the average of  $D_t$  (displacement field for top layer) and  $D_b$  (displacement field for bottom layer) causes asymmetry of the localized electron energies and creates band gap opening.<sup>24</sup> Figure 12(b) represents the variation of energy band gap versus mean value of displacement fields ( $D_{mean} = 1/2(D_t + D_b)$ ) from numerous dual-gate electrode experimental results<sup>41–43</sup> and some reported in the literature using molecular doping<sup>44,45</sup> and an internal built-in electric field which is acquired from this study. In view of Figure 12, the energy gap in bilayer graphene which is produced by the TMA layer as a p-type dopant is consistent with experimental achievements in dual gate electronic devices. The differences between the values of the fields stem from the screening of adsorbate and the

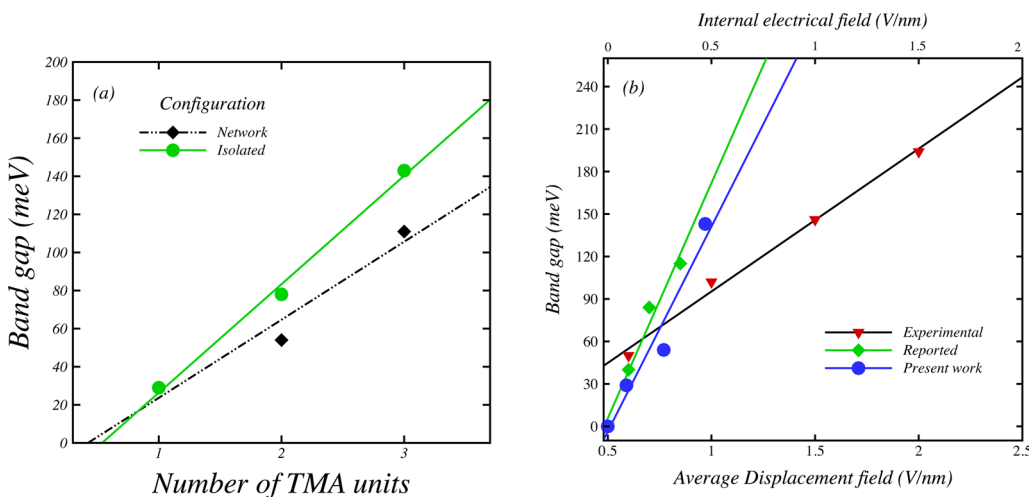


**Figure 12.** (a) Band gap–number plot of trimesic acid (TMA) and (b) variation of band gap as a function of built-in electric field  $E_{bi}$  by p-type dopant reported (green),<sup>24</sup> present work (blue), and experimental results (red).<sup>40</sup>

displacement fields in bilayer graphene which is the main issue of significant research.<sup>35,46</sup>

#### IV. CONCLUSIONS

Electronic structure properties of an organic molecule, trimesic acid adsorbed on bilayer graphene, for both the single-molecule and self-assembled layer on bilayer graphene are investigated by means of *ab initio* computations. The growth of TMA on bilayer graphene in two chicken-wire and super-flower patterns has different perturbation effects on structural stability and potential substrate. This distinction originated from different charge transfer between two layers of BLG, and this asymmetry of top and bottom layer yields to a built-in electric field between them and as a result band gap opening. The internal electrical field between the top and bottom layer ( $E_{bi}$ ) by large number of TMA (isolated trimer) doping reaches  $0.42 \text{ V}/\text{\AA}$ , along the  $k$ -point separation  $\Delta E_k = 147 \text{ meV}$  and direct gap opening  $E_g = 143 \text{ meV}$ . Moreover, our DFT results determine that with increasing of number of p-dopant TMA molecules on bilayer graphene the induced band gap increases linearly in consistency with experiment, and these findings (tuning of band gap) improve and pave the way for graphene-based nanoelectronics devices such as transistors.

#### ■ AUTHOR INFORMATION

##### Corresponding Author

\*E-mail: shayegan-far.farzaneh@polymtl.ca.

##### Notes

The authors declare no competing financial interest.

#### ■ ACKNOWLEDGMENTS

This work was supported by the Natural Sciences and Engineering Research Council of Canada (NSERC) and the Ministère du Développement économique, de l'Innovation et de l'Exportation (MDEIE) through the PSR-SIIRI program. Computational resources were provided by Calcul Québec and Compute Canada. I am grateful to prof. Alain Rochefort for all I have learned from him.

#### ■ REFERENCES

- Jong Yu, W.; Duan, X. Tunable Transport Gap in Narrow Bilayer Graphene Nanoribbons. *Sci. Rep.* **2013**, *3*, 1248.
- Wang, F.; Yu, Z.; Liu, V.; Raman, A.; Cui, Y.; Fan, S. Light Trapping in Photonic Crystals. *Energy Environ. Sci.* **2008**, *320*, 206–209.
- Xia, F.; Mueller, T.; Lin, Y.-M.; Valdes-Garcia, A. and Avouris, Ph. Ultrafast Graphene Photodetector. *Nat. Nanotechnol.* **2009**, *4*, 839–843.
- Han, M. Y.; Brant, J. C.; Kim, P. Electron Transport in Disordered Graphene Nanoribbons. *Phys. Rev. Lett.* **2010**, *104*, 056801.
- Gunlycke, D.; Areshkin, D. A.; White, C. T. Semiconducting Graphene Nanostrips with Edge Disorder. *Appl. Phys. Lett.* **2007**, *90*, 142104.
- Lherbier, A.; Blanca, B.; Yann-Michel, N.; Stephan, R. Transport Length Scales in Disordered Graphene-Based Materials: Strong Localization Regimes and Dimensionality Effects. *Phys. Rev. Lett.* **2008**, *100*, 036803.
- Evaldsson, M.; Zozoulenko, I. V.; Xu, H.; Heinzel, T. Edge-Disorder-Induced Anderson Localization and Conduction Gap in Graphene Nanoribbons. *Phys. Rev. B* **2008**, *78*, 161407(R).
- Querlioz, D.; Zozoulenko, I. V.; Xu, H.; Heinzel, T. Suppression of the Orientation Effects on Bandgap in Graphene Nanoribbons in the Presence of Edge Disorder. *Appl. Phys. Lett.* **2008**, *92*, 042108.
- Mucciolo, E. R.; Castro Neto, A. H.; Lewenkopf, C. H. Conductance Quantization and Transport Gaps in Disordered Graphene Nanoribbons. *Phys. Rev. B* **2009**, *79*, 075407.
- Martin, I.; Blanter, Y. M. Transport in Disordered Graphene Nanoribbons. *Phys. Rev. B* **2009**, *79*, 235132.
- Han, M. Y.; Ozyilmaz, B.; Zhang, Y.; Kim, P. Energy Band-Gap Engineering of Graphene Nanoribbons. *Phys. Rev. Lett.* **2007**, *98*, 206805.
- Li, X.; Wang, X.; Zhang, L.; Lee, S.; Dai, H. Chemically Derived, Ultrasmooth Graphene Nanoribbon Semiconductors. *Science* **2008**, *319*, 1229–1232.
- Bai, J.; Duan, X.; Huang, Y. Rational Fabrication of Graphene Nanoribbons Using a Nanowire Etch Mask. *Nano Lett.* **2009**, *9*, 2083–2087.
- Wang, X.; Dai, H. Etching and Narrowing of Graphene from the Edges. *Nat. Chem.* **2010**, *2*, 661–665.
- Bai, J.; Zhong, X.; Jiang, S.; Huang, Y.; Duan, X. Graphene Nanomesh. *Nat. Nanotechnol.* **2010**, *5*, 190–194.
- Zhang, Y.; Tang, T.-T.; Girit, C.; Hao, Z.; Martin, M. C.; Zettl, A.; Crommie, M. F.; Shen, Y. R.; Wang, F. Direct Observation of a Widely Tunable Bandgap in Bilayer Graphene. *Nature* **2009**, *459*, 820–823.
- Castro, E. V.; Novoselov, K. S.; Morozov, S. V.; Peres, N. M. R.; Lopes dos Santos, J. M. B.; Nilsson, J.; Guinea, F.; Geim, A. K.; Castro

- Netoet, A. H. Biased Bilayer Graphene: Semiconductor with a Gap Tunable by the Electric Field Effect. *Phys. Rev. Lett.* **2007**, *99*, 216802.
- (18) Ohta, T.; Bostwick, A.; Seyller, Th.; Horn, K.; Rotenberg, E. Controlling the Electronic Structure of Bilayer Graphene. *Science* **2006**, *313*, 951–954.
- (19) Xia, F.; Farmer, D. B.; Lin, Y. and Avouris, Ph. Graphene Field-Effect Transistors with High On/Off Current Ratio and Large Transport Bandgap at Room Temperature. *Nano Lett.* **2010**, *10*, 715–718.
- (20) Yu, W. J.; Liao, L.; Chae, S. H.; Lee, Y. H.; Duan, X. Toward Tunable Bandgap and Tunable Dirac Point in Bilayer Graphene with Molecular Doping. *Nano Lett.* **2011**, *11*, 4759–4763.
- (21) Choi, S.-M.; Jhi, S.-H.; Son, Y.-W. Controlling Energy Gap of Bilayer Graphene by Strain. *Nano Lett.* **2010**, *10*, 3486–3489.
- (22) Samarakoon, D. K.; Wang, X. Q. Tunable Band Gap in Hydrogenated Bilayer Graphene. *ACS Nano* **2010**, *4*, 4126–4130.
- (23) Tian, X.; Xu, J. B.; Wang, X. Band Gap Opening of Bilayer Graphene by F4-TCNQ Molecular Doping and Externally Applied Electric Field. *J. Phys. Chem. B* **2010**, *114*, 11377–11381.
- (24) Samuels, A. J.; Carey, J. D. Molecular Doping and Band-Gap Opening of Bilayer Graphene. *ACS Nano* **2013**, *7*, 2790–2799.
- (25) Mak, K.; Lui, C.; Shan, J.; Heinz, T. Observation of an Electric Field Induced Band Gap in Bilayer Graphene by Infrared Spectroscopy. *Phys. Rev. Lett.* **2009**, *102*, 100–103.
- (26) Shayeganfar, F.; Rochefort, A. Electronic Properties of Self-Assembled Trimesic Acid Monolayer on Graphene. *Langmuir* **2014**, *30*, 9707–9716.
- (27) Lackinger, M.; Heckl, W. M. Carboxylic Acids: Versatile Building Blocks and Mediators for Two-Dimensional Supramolecular Self-Assembly. *Langmuir* **2009**, *25*, 11307–11321.
- (28) Soler, J. M.; Artacho, E.; Gale, J. D.; García, A.; Junquera, J.; Ordejón, P.; Sánchez-Portal, D. The SIESTA Method for Ab Initio Order-N Materials Simulation. *J. Phys.: Condens. Matter* **2002**, *14*, 2745–2779.
- (29) Vosko, S. H.; Wilk, L.; Nusair, M. Accurate Spin-Dependent Electron Liquid Correlation Energies for Local Spin Density Calculations: A Critical Analysis. *Can. J. Phys. (Paris)* **1980**, *58*, 1200.
- (30) Partoens, B.; Peeters, F. M. From Graphene to Graphite: Electronic Structure around the K Point. *Phys. Rev. B* **2006**, *74*, 075404.
- (31) Janta-Polczynski, B.; Cerdá, J. L.; Éthier-Majcher, G.; Piyakis, K.; Rochefort, A. Parallel Scanning Tunneling Microscopy Imaging of Low Dimensional Nanostructures. *J. Appl. Phys.* **2008**, *104*, 023702.
- (32) Boulanger-Lewandowski, N.; Rochefort, A. Intrusive STM Imaging. *Phys. Rev. B* **2011**, *83*, 115430.
- (33) Landrum, G. YAeHMOP; Yet Another Extended Hückel Molecular Orbital Package; Cornell University: Ithaca, NY, 1995.
- (34) Tersoff, J.; Hamann, D. R. Theory and Application for the Scanning Tunneling Microscope. *Phys. Rev. Lett.* **1983**, *50*, 1998.
- (35) McCann, E. Asymmetry Gap in the Electronic Band Structure of Bilayer Graphene. *Phys. Rev. B* **2006**, *74*, 161403.
- (36) Min, H.; Sahu, B.; Banerjee, S. K.; MacDonald, A. H. Ab Initio Theory of Gate Induced Gaps in Graphene Bilayers. *Phys. Rev. B* **2007**, *75*, 155115.
- (37) Griessl, S.; Lackinger, M.; Edelwirth, M.; Hietschold, M.; Heckl, W. M. Self-Assembled Two-Dimensional Molecular Host-Guest Architectures from Trimesic Acid. *Single Mol.* **2002**, *3*, 25–31.
- (38) Lackinger, M.; Griessl, S.; Heckl, W. M.; Hietschold, M.; Flynn, W. Self-Assembly of Trimesic Acid at the Liquid-Solid Interface—a Study of Solvent-Induced Polymorphism. *Langmuir* **2005**, *21*, 4984–4988.
- (39) Balog, R.; Jørgensen, B.; Nilsson, L.; Andersen, M.; Rienks, E.; Bianchi, M.; Fanetti, M.; Lægsgaard, E.; Baraldi, A.; Lizzit, S. Bandgap Opening in Graphene Induced by Patterned Hydrogen Adsorption. *Nat. Mater.* **2010**, *9*, 315–319.
- (40) Zhang, Y.; Tang, T.-T.; Girit, C.; Hao, Z.; Martin, M. C.; Zettl, A.; Crommie, M. F.; Shen, Y. R.; Wang, F. Direct Observation of a Widely Tunable Band Gap in Bilayer Graphene. *Nature* **2009**, *459*, 820–823.
- (41) Panchakarla, L. S.; Subrahmanyam, K. S.; Saha, S. K.; Govindaraj, A.; Krishnamurthy, H. R.; Waghmare, U. V.; Rao, C. N. R. Synthesis, Structure, and Properties of Boron- and Nitrogen-Doped Graphene. *Adv. Mater.* **2009**, *21*, 4726–4730.
- (42) Szafranek, B. N.; Schall, D.; Otto, M.; Neumaier, D.; Kurz, H. High On/Off Ratios in Bilayer Graphene Field Effect Transistors Realized by Surface Dopants. *Nano Lett.* **2011**, *11*, 2640–2643.
- (43) Xia, F.; Farmer, D. B.; Lin, Y.; Avouris, P. Graphene Field-Effect Transistors with High On/Off Current Ratio and Large Transport Band Gap at Room Temperature. *Nano Lett.* **2010**, *10*, 715–718.
- (44) Duong, D. L.; Lee, S. M.; Chae, S. H.; Ta, Q. H.; Lee, S. Y.; Han, G. H.; Bae, J. J.; Lee, Y. H. Band-Gap Engineering in Chemically Conjugated Bilayer Graphene: Ab Initio Calculations. *Phys. Rev. B* **2012**, *85*, 205413.
- (45) Cuong, N. T.; Otani, M.; Okada, S. Electron-State Engineering of Bilayer Graphene by Ionic Molecules. *Appl. Phys. Lett.* **2012**, *101*, 233106.
- (46) Gava, P.; Lazzeri, M.; Saitta, A.; Mauri, F. Ab Initio Study of Gap Opening and Screening Effects in Gated Bilayer Graphene. *Phys. Rev. B* **2009**, *79*, 165431.